

DiffXPBD : Differentiable Position-Based Simulation of Compliant Constraint Dynamics

TUUR STUYCK, Meta Reality Labs Research, USA

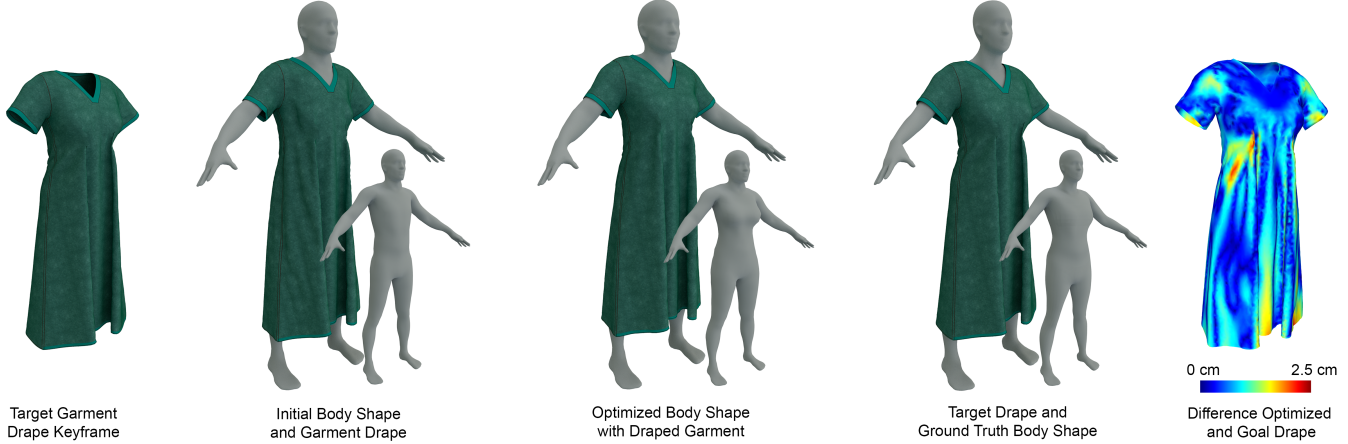


Fig. 1. We present a fully analytically differentiable solver that allows to obtain gradients with respect to a desired parameter in order to minimize a goal function. In this example, we show how coefficients for the shape of a statistical body model can efficiently be computed in order to minimize the distance of the draped clothing to an observed reference. Our differentiable solver can differentiate through collisions of the cloth with the underlying body shape which allows the gradient information to propagate. Left shows the target drape. Next, we show the original body shape with the draped cloth. The middle figure shows the final optimized body shape that produces a drape close to the goal shape. The goal drape and ground truth body shape are shown second to the right. The rightmost figure visualizes the distance of the estimated garment drape to the ground truth drape. Note how they closely coincide where the garment touches the body, indicating a successful optimization result.

We present DiffXPBD, a novel and efficient analytical formulation for the differentiable position-based simulation of compliant constrained dynamics (XPBD). Our proposed method allows computation of gradients of numerous parameters with respect to a goal function simultaneously leveraging a performant simulation model. The method is efficient, thus enabling differentiable simulations of high resolution geometries and degrees of freedom (DoFs). Collisions are naturally included in the framework. Our differentiable model allows a user to easily add additional optimization variables. Every control variable gradient requires the computation of only a few partial derivatives which can be computed using automatic differentiation code. We demonstrate the efficacy of the method with examples such as elastic material parameter estimation, initial value optimization, optimizing for underlying body shape and pose by only observing the clothing, and optimizing a time-varying external force sequence to match sparse keyframe shapes at specific times. Our approach demonstrates excellent efficiency and we demonstrate this on high resolution meshes with optimizations involving over 26 million degrees of freedom. Making an existing solver differentiable requires only a few modifications and the model is compatible with both modern CPU and GPU multi-core hardware.

CCS Concepts: • Computing methodologies → Physical simulation.

Additional Key Words and Phrases: differentiable simulation, parameter estimation

1 INTRODUCTION

Clothing is an essential part of our daily lives. This holds true for our virtual selves with applications such as virtual try-on, digital humans, and avatars. Physics-based simulations methods for cloth have shown widespread success across several domains including computer graphics and visual effects over the last decades and many different techniques have been proposed. The seminal work of Baraff and Witkin [1998] introduced an implicit integration scheme enabling, for the first time, simulations with large time steps which remain stable and result in efficient simulations. This method is still commonly used in top-tier animation studios [Kim and Eberle 2022]. Since then, many novel approaches have been proposed to tackle different shortcomings. The introduction of Position Based Dynamics (PBD) [Müller et al. 2007] enabled a unified high performance solver that maps efficiently to modern parallel hardware such as multi-core CPUs and GPUs. Follow up work introduced eXtended Position Based Dynamics (XPBD) [Macklin et al. 2016] which resolves the iteration and time step dependent stiffness issue of PBD. Project Dynamics (PD) [Bouaziz et al. 2014] introduced a fast local-global solver for implicit time integration of FEM simulations with elastic energies in a quadratic form. Stuyck [2018] provides an overview of several cloth simulation techniques.

However, even though these simulations can be made visually indistinguishable from reality, it is the result of a laborious iterative

process requiring expert users. On the other hand, data-driven methods have shown to produce detailed results but do not generalize as well as simulation models. With the proliferation of machine learning and data-driven techniques, there has been a renewed interest in the exploration of differentiable solvers in the optimization loop for a multitude of tasks such as model identification, material estimation, inverse design, and optimization. Differentiable simulation will act as key component to bridge physics and data-driven approaches. Additionally, recent advances in cloth capture systems [Chen et al. 2021; Halimi et al. 2022; White et al. 2007] provide high quality data that can be used for learning the simulation parameters. The idea of fine-tuning a physics-based simulation model to data is a powerful concept that uses real data and, once fitted, provides a generalizable model. This has the potential to reduce the need for artist-in-the-loop for fine-tuning simulations and automated parameter estimation pipelines.

It is essential to enable efficient gradient computation. We are the first to present an analytical differentiable formulation for the XPBD simulation framework. Our method naturally includes collisions, enabling an efficient differentiable unified simulation model with contact. The differentiable solver can easily be extended to novel constraints by adding only a few partial derivatives per constraint.

Our contributions are the following :

- We present a differentiable formulation for position-based simulation of compliant constraint dynamics. The method is efficient, scales to large number of DoFs, and maintains all advantages of the forward simulation model.
- Our method naturally handles cloth self-collisions and collisions with the environment which enables gradient propagation through these collisions.
- The approach requires only a small addition to the forward simulation model and as such, it can be easily added to existing solvers. The backward solve can be implemented using off-the-shelf tools.
- The system operates on sparse matrices, resulting in limited memory usage. Intermediate data can be stored and retrieved when needed.

We demonstrate the efficacy of the method for a variety of tasks. We show that our method is capable of efficiently computing derivatives of high DoFs and high geometric resolutions.

2 RELATED WORK

We review methods of differentiable simulation models and their applications with a focus on the simulation of elastic deformables.

Differentiable Simulation has been investigated in recent research [Liang et al. 2019; Qiao et al. 2020] for system identification and for inferring material parameters from observations [Hu et al. 2019; Strecke and Stücker 2021]. It has applications in computer graphics, vision, robotics and many others. Several of these techniques rely on the adjoint method for gradient computation. Over the last decades, the adjoint method has been successfully applied to differentiate various dynamic simulation models. This includes fluid simulation [McNamara et al. 2004] and implicit simulation of cloth dynamics [Wojtan et al. 2006]. The adjoint method continues to be

successfully applied with a focus on time-dependent deformation problems with contact [Gjoka et al. 2022]. Notoriously, cloth simulations frequently undergo numerous contacts. Because of this, work has focused specifically on the handling of differentiable simulation in contact heavy scenarios. Liang et al. [2019] introduced a differentiable approach for handling cloth collisions using a linear complementary problem but the method was only demonstrated to work with low resolution meshes and sparse contact. Du et al. [2021] introduced a differentiable approach to Project Dynamics using the adjoint method, enabling fast differentiable simulations. Follow up work extends this line of research to handle contact [Li et al. 2022] with a specific application to cloth simulations supporting dry frictional contact. Coros et al. [2021] provide an overview of differentiable simulation methods.

Differentiable soft body simulation models [Geilinger et al. 2020; Hahn et al. 2019] and estimating material properties of scanned volumetric objects using differentiable simulation as an inverse design problem has been active domain of research [Weiss et al. 2020]. Chen et al. [2022] introduced differentiable point based simulation for material estimation of soft deformable bodies coupled with neural radiance field representations [Mildenhall et al. 2021]. Similarly, parameter estimation for cloth simulations has been a focus of attention [Larionov et al. 2022; Miguel et al. 2012; Wang et al. 2011]. Guo et al. [2021] showed that is possible to estimate body shape and pose given a point cloud by differentiating through clothing simulations. A full end-to-end system is presented by Jatavallabhula et al. [Jatavallabhula et al. 2021]. They propose a system identification technique by combining differentiable simulation with differentiable rendering which allows them to backpropagate gradient information from pixels in a video sequence. This pipeline enables them to optimize for control variables to reproduce image observations directly. Other simulation models like the Material Point Method have successfully been made differentiable [Hu et al. 2019] and have been used for a variety of control tasks [Hu et al. 2020].

In addition to analytical formulations of these differentiable simulation models, specialized differentiable programming frameworks focusing on physics-based simulation applications are becoming more commonplace [Hu 2022; Macklin 2022].

In summary, the research field has made great progress enabling dynamic differentiable simulation for several applications. However, several issues still remain. Performance and memory usage is a primary concern for any differentiable method because many of these simulations need to be computed to iteratively optimize a goal function. Prior work has been limited to low or medium geometric resolutions. With our efficient and highly parallelizable formulation, we demonstrate optimizations involving high resolution geometries and DoFs.

3 BACKGROUND

The method uses position-based simulation of compliant constraint dynamics, also known as eXtended Position Based Dynamics as the

simulation model and the adjoint method to efficiently differentiate through it. We briefly review both here.

3.1 XPBD: Position-Based Simulation of Compliant Constrained Dynamics

XPBD is an efficient unified simulation model, capable of producing real-time simulations. The constraint-based formulation can be parallelized [Fratarcangeli et al. 2016] and implemented on modern GPU and multi-core CPU hardware. As a result, the model showcases much better performance compared to expensive non-linear solvers. The method solves Newton’s equations of motion given by $\mathbf{M}\ddot{\mathbf{x}} = -\nabla U^\top(\mathbf{x})$, where \mathbf{x} are the vertex positions and \mathbf{M} is the mass matrix. The energy potential $U(\mathbf{x})$ is formulated in terms of a vector of constraint functions $\mathbf{C} = [C_1(\mathbf{x}), \dots, C_m(\mathbf{x})]^\top$ and inverse compliance matrix $\boldsymbol{\alpha}^{-1}$ as

$$U(\mathbf{x}) = \frac{1}{2} \mathbf{C}(\mathbf{x})^\top \boldsymbol{\alpha}^{-1} \mathbf{C}(\mathbf{x}), \quad (1)$$

Implicit Euler time integration results in the constraint multiplier updates $\Delta\lambda$ being computed as

$$(\nabla \mathbf{C}(\mathbf{x}_i)^\top \mathbf{M}^{-1} \nabla \mathbf{C}(\mathbf{x}_i) + \tilde{\boldsymbol{\alpha}}) \Delta\lambda = -\mathbf{C}(\mathbf{x}_i) - \tilde{\boldsymbol{\alpha}} \lambda_i, \quad (2)$$

where $\tilde{\boldsymbol{\alpha}} = \boldsymbol{\alpha}/\Delta t^2$. Given $\Delta\lambda$, the position update is computed as

$$\Delta\mathbf{x} = \mathbf{M}^{-1} \nabla \mathbf{C}(\mathbf{x}_i) \Delta\lambda. \quad (3)$$

3.2 The Adjoint Method

The gradients $d\phi/du$ required to minimize a goal function ϕ with respect to control variables \mathbf{u} are typically intractable to compute directly for dynamic simulations. The adjoint method provides an efficient solution to compute these derivatives by modifying the problem so that only partial derivatives, which are more easily computed, are needed. The gradients of the control variables with respect to some goal function can be computed as

$$\frac{d\phi}{du} = \frac{\partial\phi}{\partial Q} \frac{dQ}{du} + \frac{\partial\phi}{\partial u} \quad (4)$$

The adjoint method turns this intractable computation into a more manageable and efficient formulation by replacing the vector-matrix product containing dQ/du in Eq. 4 with an equivalent computation involving the adjoint of Q . We refer to Wojtan et al. [2006] for an in-depth overview. The simulation moves the states forward in time using $Q = F(Q, \mathbf{u})$. The resulting equations then become

$$\frac{d\phi}{du} = \hat{Q}^\top \frac{\partial F}{\partial u} + \frac{\partial\phi}{\partial u} \quad (5)$$

where the adjoint states \hat{Q} are computed in a backward pass using

$$\hat{Q} = \left(\frac{\partial F}{\partial Q} \right) \hat{Q} + \left(\frac{\partial\phi}{\partial Q} \right)^\top \quad (6)$$

Using this approach, we are able to compute many gradients simultaneously in a single forward-backward pass at the cost of needing to store intermediate quantities. In practice, this is a good trade-off since these quantities do not need to be kept in ram memory and thus the method is feasible on memory limited-devices. Only a small subset of the data is needed during a single adjoint

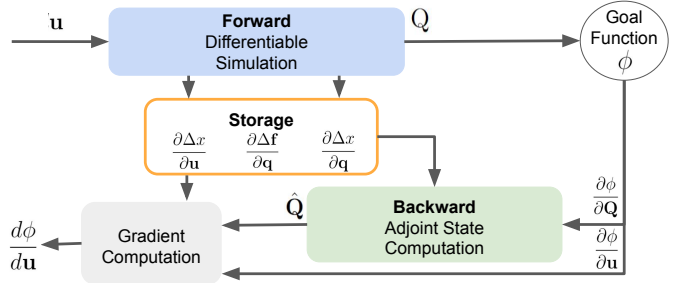


Fig. 2. Overview of the different components of the gradient computation process. We perform a forward simulation during which we compute and store the quantities required in the backward pass. After completing the forward simulation, the goal function gets evaluated which in turn starts the backward adjoint state computation pass. Once the adjoint states have been computed, the total gradient $d\phi/du$ can be obtained.

state computation step. This is in contrast to automatic differentiation frameworks where the computational graph can become exceedingly large.

4 METHOD

The method can be thought of as a two-step process involving a forward and a backward simulation as illustrated in Figure 2. In the forward step, we perform a simulation where for every step, we compute additional derivatives that are stored. In the backward pass, we perform a backward simulation which computes the adjoint states \hat{Q} . This requires the stored derivatives from the forward pass to assemble the sparse linear system. At the end of this pass we have all the required quantities to compute the full derivative of the goal function ϕ with respect to the desired control variables \mathbf{u} as stated in Eq. 5.

4.1 Adjoint State Computation

We find the backward adjoint computation pass by applying Eq. 6 to the XPBD simulation scheme. After some re-arranging and by substituting \hat{v}_n we find

$$\left(I - \frac{\partial \Delta x}{\partial x} - \Delta t^2 M^{-1} \frac{\partial f}{\partial x} - \frac{1}{\Delta t} \frac{\partial \Delta x}{\partial v} - \Delta t M^{-1} \frac{\partial f}{\partial v} \right)^\top \hat{x}_n = \hat{x}_{n+1} + \frac{\partial \phi}{\partial x_n} \quad (7)$$

where f denotes forces that are applied directly to the velocity and are not solved for in a constraint. We make the system matrix symmetric by left multiplying with the mass matrix M and solving this sparse symmetric linear system using Conjugate Gradients (CG) to obtain \hat{x}_n . We directly find $\hat{v}_n = \Delta t \hat{x}_n + \partial \phi / \partial v_n$.

4.1.1 Linear System Filtering. Vertices are often fully constrained in the simulation due to Dirichlet boundary conditions. These pinned vertices are modeled using an infinite mass. To handle this in a robust manner, we rely on modified Conjugate Gradient with pre-filtering as presented by Tamstorf et al. [2015].

4.2 Goal Function

Our aim is to minimize a goal function ϕ by modifying the control variables \mathbf{u} . This function can be easily provided by the user and adapted based on the problem at hand. The most straight-forward metric is to compare simulation state \mathbf{Q} directly with a given reference \mathbf{Q}^* using

$$\phi(\mathbf{u}, \mathbf{Q}) = \frac{1}{2} \sum_{n=0}^N \left(\|\mathbf{W}_n(\mathbf{q}_n - \mathbf{q}_n^*)\|^2 + \beta \|\mathbf{u}_n\|^2 \right) \quad (8)$$

where a regularization term with weight β based on the control variable \mathbf{u} had been added. The weight matrix \mathbf{W}_n can be used to introduce relative importance. The goal function can be defined over all frames N or a subset thereof. Any goal function or combination of goal functions can be used as long as the required derivatives $\partial\phi/\partial\mathbf{q}$ and $\partial\phi/\partial\mathbf{u}$ can be computed. Section 6.2 shows the use of a point cloud based goal function.

4.3 Control Variable Derivative Computation

For every control variable \mathbf{u} we wish to obtain a gradient for, we need to compute and store $\partial\Delta\mathbf{x}/\partial\mathbf{u}$. This, in combination with the previously computed adjoint states, allow us to evaluate Eq. 5 which provides us with the full gradient $d\phi/d\mathbf{u}$. Note, we can compute several different control variables simultaneously and we do not require a separate forward-backward pass for each.

4.4 Position Update Derivative Computation

For every constraint in the system, we will need to differentiate through the position update $\Delta\mathbf{x}$ in order to obtain $\partial\Delta\mathbf{x}/\partial\mathbf{x}$ and $\partial\Delta\mathbf{x}/\partial\mathbf{u}$. These derivatives can be computed using several approaches such as analytically or using automatic or symbolic differentiation techniques. The derivatives can be accumulated in parallel in the same iterative fashion as the position updates themselves, which allows the method to remain highly performant and parallelizable.

4.4.1 Derivative Verification. Regardless of the method of computation, one can check the properties documented by Kim and Eberle [2022] to validate the derivatives. In XPBD, the force from an elastic potential is given as $\mathbf{f} = -\nabla_{\mathbf{x}} U^T(\mathbf{x}_{n+1})$ and therefore the force derivative blocks $\partial\mathbf{f}/\partial\mathbf{x}$ can be directly obtained from the position update derivative blocks $\partial\Delta\mathbf{x}/\partial\mathbf{x}$. The column blocks of the derivative should sum to zero and the row blocks by symmetry as well. Additionally, we can verify $\partial\mathbf{f}_i/\partial\mathbf{x}_j = \partial\mathbf{f}_j^T/\partial\mathbf{x}_i$.

4.4.2 Positive Definite Projection. The backward pass requires a linear system solve of a large symmetric sparse system. Although a direct solver can be used, iterative solvers like Preconditioned Conjugate Gradients (PCG) are preferred due to its efficiency. PCG requires the matrix to be semi-positive-definite. Additionally, a system that is not semi-positive-definite implies the existence of multiple solutions which will lead to instabilities [Kim and Eberle 2022]. Therefore, we project all derivative blocks to positive definiteness by clamping the eigenvalues from the eigen decomposition. This only happens once at the end of each simulation step. The projection step is efficient as it can be computed in parallel over all derivatives simultaneously.

4.5 Collision Handling

In order to include collision handling in our differentiable framework, we use stiff spring constraints to maintain a closest separation distance of at least a user-set thickness between the garment layers as well as the body surface. We use spring constraints over hard discontinuous constraints to obtain smooth gradient flow. The approach is compatible with any collision detection strategy such as continuous time collision detection.

5 EXAMPLE APPLICATIONS

Our method provides an easy way to efficiently compute gradients analytically with respect to any control variable. To illustrate this, we present several optimization example applications leveraging our pipeline. Our method is not limited to these specific examples.

5.1 Material Parameter Estimation

We demonstrate cloth material parameter optimization. We use an orthotropic Saint Venant-Kirchhoff membrane energy model combined with a discrete bending [Bender et al. 2017] term to model the fabric properties. Different material models are equally applicable and our proposed differentiation method is not limited to these. Per triangle with area A , the membrane model has an inverse compliance matrix of the form

$$\boldsymbol{\alpha}_{\Delta}^{-1} = A \begin{bmatrix} C_{00} & C_{01} & & \\ C_{01} & C_{11} & & \\ & & & \\ & & & C_{22} \end{bmatrix},$$

where C_{ij} are the compliance coefficients. The constraint function for each triangle is then defined to be the Green strain ϵ in Voigt notation $\mathbf{C}_{\Delta}(\mathbf{x}) = (\epsilon_{uu}, \epsilon_{vv}, 2\epsilon_{uv})^T$, where subscripts u and v indicate warp and weft directions, respectively. The out-of-plane bending constraint is defined for each pair of triangles sharing a dihedral edge $(\mathbf{x}_1, \mathbf{x}_3, \mathbf{x}_2), (\mathbf{x}_1, \mathbf{x}_2, \mathbf{x}_4)$ as the angle strain

$$C_{\text{bend}} = \arccos \left(\frac{\mathbf{x}_{2,1} \times \mathbf{x}_{3,1}}{\|\mathbf{x}_{2,1} \times \mathbf{x}_{3,1}\|} \cdot \frac{\mathbf{x}_{2,1} \times \mathbf{x}_{4,1}}{\|\mathbf{x}_{2,1} \times \mathbf{x}_{4,1}\|} \right) - \phi_0,$$

The rest dihedral angle is denoted by ϕ_0 and $\mathbf{x}_{i,j} = \mathbf{x}_i - \mathbf{x}_j$ are edge vectors between vertices i and j . The inverse compliance matrix is given by the scalar bending stiffness: $\boldsymbol{\alpha}_{\text{bend}}^{-1} = b$.

We optimize directly over the compliance coefficients and bending parameter by choosing the parameter set to be

$$\gamma := (C_{00}, C_{11}, C_{01}, C_{11}, b), \gamma \in \Gamma, \quad (9)$$

where the parameters are constrained to be in the feasible set Γ . In order to optimize for these parameters, we compute and store $\partial\Delta\mathbf{x}/\partial\gamma$ during the constraint solve at every step.

5.2 Body Shape Optimization

Given a statistical body model such as SMPL [Loper et al. 2015] but not limited to this specific model, we can estimate the PCA shape coefficients α that would minimize a given goal function defined on the simulated cloth mesh. The connection between the cloth and the body is established through the collisions and gradients can flow through freely. We accumulate gradients with respect to the

	Shirt	T-shirt	Dress	Pants	Swatch	Body
Vertices	65,968	14,639	10,422	8002	441	7,324
Faces	131,421	29,032	20,685	16,170	800	14,644

Table 1. Mesh resolutions used in the examples.

coefficients using the chain rule

$$\frac{\partial \Delta \mathbf{x}_{\text{cloth-body collision}}}{\partial \alpha} = \frac{\partial \Delta \mathbf{x}_{\text{cloth-body collision}}}{\partial \mathbf{x}_{\text{body}}} \frac{\partial \mathbf{x}_{\text{body}}}{\partial \alpha}$$

5.3 Skeleton Pose Optimization

Similarly as for the body shape optimization, by applying the chain rule and differentiating through the linear blend skinning directly, we obtain the gradient with respect to the skeleton joint angles τ using

$$\frac{\partial \Delta \mathbf{x}_{\text{cloth-body collision}}}{\partial \tau} = \frac{\partial \Delta \mathbf{x}_{\text{cloth-body collision}}}{\partial \mathbf{x}_{\text{body}}} \frac{\partial \mathbf{x}_{\text{body}}}{\partial \tau}$$

5.4 Initial Value Optimization

Following Equation 5, the gradient with respect to the initial position and velocities can be directly obtained from the adjoint states.

5.5 Keyframe Simulation

The method can also be used for motion in-betweening or stitching distinct simulations together. Provided with a few keyframes, the method can automatically optimize for an external time-varying force sequence that pushes the clothing through the keyframes at the desired times. We optimize directly for all external forces per particle per step resulting in a high dimensional optimization problem. The external force gradients can be directly obtained from the adjoint velocities.

6 RESULTS

We demonstrate the efficacy of our method with respect to several applications. All differentiable simulations are dynamic and accompanying videos can be found in the supplemental material. The resolutions of the garments are reported in Table 1.

6.1 Material Parameter Estimation

We demonstrate estimation of the bending stiffness for a dress draped on a static body in Figure 3. Our method is capable of optimizing the material parameter while the clothing is draped into a body for which the collisions are taken into account in the backward step. Similarly, we estimate in-plane elastic material properties. Figure 4 demonstrates the optimization of the Young’s moduli in both warp and weft direction such that a target shape gets matched at a specific frame in a dynamic simulation. In this example, all triangles in the swatch share the same material.

6.2 Body Shape Optimization

We show that it is possible to optimize for the coefficients of an underlying statistical body model so that a draped garment would

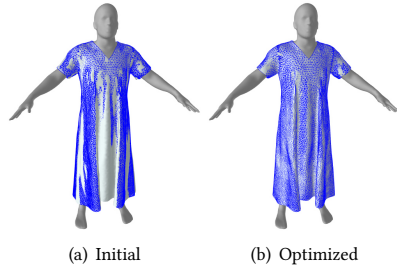


Fig. 3. *Bend Stiffness Optimization on Body.* Material parameter estimation is effective even when the clothing is interacting with an underlying body. Notice how the optimized fabric coincides closely with the target shape shown in the blue wireframe.

match a given cloth observation as closely as possible. This is demonstrated in Figure 1. In this example, we optimize for all 2781 body PCA coefficients directly. All gradients are computed simultaneously in a single forward-backward pass.

In Figure 5, we show that it is even possible to optimize body shape for a scan of a real person captured wearing a t-shirt. Since the scan has a different topology than the simulated garment, we use a goal function based on the closest distance of the simulated vertices to the scan where closest points computations are recomputed every iteration and the t-shirt geometry is segmented out of the scan. The segmented t-shirt scan contains 144,556 vertices and 288,034 faces.

6.3 Skeleton Pose Optimization

We can optimize for the skeleton pose that through a linear blend skinning operation defines the body surface positions. We show that we can optimize this pose to produce a draped garment that matches the reference closely. Different iteration results of this experiment are shown in Figure 6.

6.4 Initial Value Optimization

We demonstrate optimizing over initial condition parameters. We intend to find the initial velocity per vertex so that at the end of the simulation, the clothing is at a specified position and pose provided by the keyframe. Figure 7 visualizes different iteration results. In the first iteration, the shirt simply falls down due to gravity. In the following iterations, the model iteratively updates the initial velocity prediction such that the shirt coincide closely with the goal shape at the requested frame. This example highlights the scalability of our method by easily estimating all 197,904 velocity values directly.

6.5 Keyframe Simulation

Given a few sparse keyframes of the cloth geometry, we want to optimize the time-varying sequence of forces so that the cloth geometry passes through the provided keyframes at the desired time. We initialize the sequence with forces equal to zero. Initially, the garment falls down under gravity but then converges to a solution where the garment flows through the desired keyframes at the requested time, see Figure 8. This example highlights the capability of our method to optimize for high number of DoFs in an efficient and scalable way. We optimize for 900 simulation steps which results in 21,605,400 control variables being optimized for simultaneously. To the best of our knowledge, this far exceeds prior work.



Fig. 4. *Young’s Moduli Optimization*. From left to right, we show different iterations of a cloth swatch draping under gravity with its corners pinned. The simulated cloth is textured and the goal shape is shown in blue. We optimize for the elastic material properties such that the simulated cloth reaches the desired pose at the requested frame. Initially, the material is too stiff and sags insufficiently under gravity to reach the target state. The optimization converges quickly to a looser material such that the cloth and target coincide at the specified frame number.

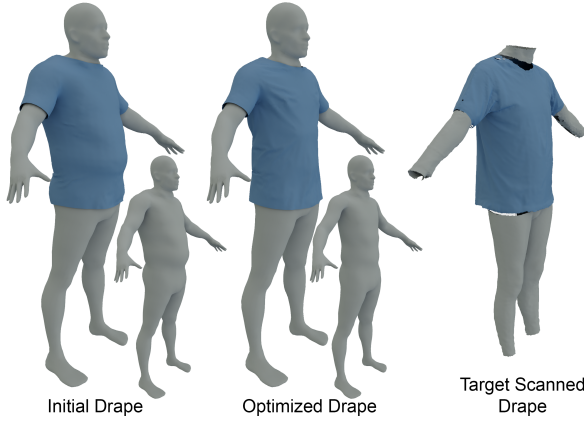


Fig. 5. *Body Shape Optimization From Scan*. We show successful body shape optimization given a scan of a real person where the target cloth geometry is high resolution and has a different topology from the simulated shirt. We optimize for all 2781 body shape PCA coefficient.

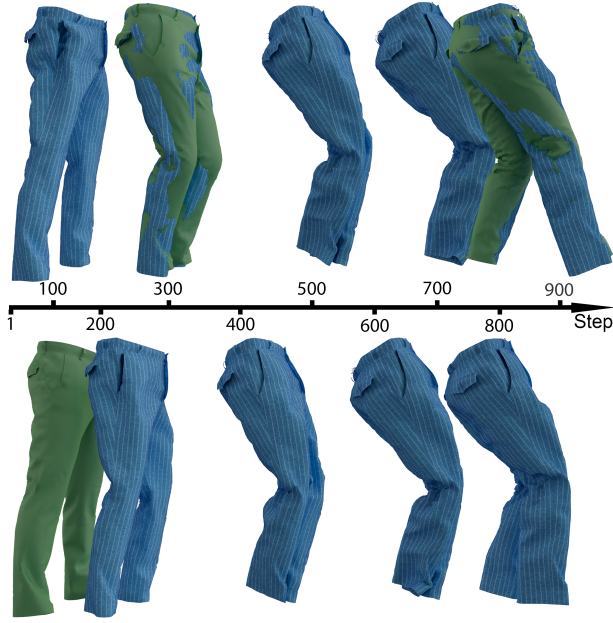


Fig. 8. *External Force Sequence Optimization*. We optimize for the time-varying force sequence that pushes the simulated garment (blue) through the keyframes (green) at the requested time. Our method is capable of handling high DoFs. In this example, over 21 million DoFs are being optimized for.

	Forward Pass		Backward Pass	
	Simulation	Differentiable Simulation	Matrix Assembly	CG Solve
Shirt	0.145	2.459	0.490	2.046
T-Shirt	0.079	0.496	0.087	0.476
Dress	0.056	0.354	0.064	0.282
Pants	0.053	0.192	0.050	0.254
Swatch	0.005	0.011	0.003	0.005

Table 2. *Timings in seconds*. The normal and differentiable forward simulation per step are listed on the left and the backward pass on the right. Timings are computed as the average per step.

	Dynamic	Resolution	DoFs	Efficiency
[Guo et al. 2021]	✗	Medium	Medium	Slow
[Wojtan et al. 2006]	✓	Low	Medium	Slow
[Liang et al. 2019]	✓	Low	Low	Slow
[Hu et al. 2019]	✓	Low	Medium	Fast
[Du et al. 2021]	✓	Medium	Medium	Fast
DiffXPBD (Ours)	✓	High	High	Fast

Table 3. *Summary of Related Work*. Our work achieves all desirable features.

6.6 Performance

We provide timing results to indicate the efficiency of our method. The algorithm is implemented using C++ on CPU and we report the timings in Table 2. All experiments are run using an AMD Ryzen Threadripper PRO 3975WX 32-Cores using 20 constraint iterations with a time step of 0.0016 ms. The timings reported include collision detection and resolving, the constraint solve, and the computation of the additional derivative terms, which includes positive definite projection. We also report the timing of the non-differentiable version of the solver. Although enabling differentiability adds some expected overhead, the method remains performant and faster than related work for similar resolutions, see Section 6.7. The backward pass consists of matrix assembly from the individual derivative blocks and the linear system solve using Conjugate Gradients.

6.7 Comparisons To Related Work

Table 3 provides a feature comparison to related work. Guo et al. demonstrates body pose and shape optimization from cloth scans. They assume that variations in the time-varying body states only affect the current state of the cloth geometry. This simplification is justified since this would require propagating gradients across the entire simulation resulting in intractable computations. Wojtan et al. presented

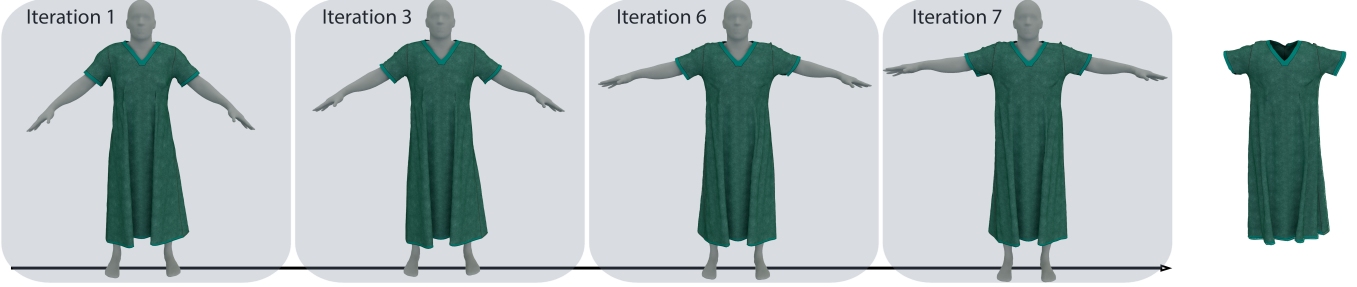


Fig. 6. *Skeleton Pose Optimization*. We show how the skeleton pose can be recovered simply by looking at the drape of the garment. From left to right, we visualize different optimization iterations and the target drape is shown on the far right. We optimize over the 3 rotational DoFs of all 114 joints simultaneously.



Fig. 7. *Initial condition optimization*. We show that our method is capable of optimizing the initial velocity per vertex in order to reach a specific pose and location at a specified frame in the simulation. The pink shirt indicates the starting position and the green is the goal position and shape. Different iterations are visualized. The inset images provide a non-occluded view of the final optimized shape per iteration. Note that our method effortlessly handles high DoFs. In this example, we compute gradients for 197,904 velocity values simultaneously.

a differentiable implicit simulator for cloth, but only demonstrated results on low resolutions and medium DoFs. Liang et al. demonstrate differentiable cloth simulation but their method is limited to low resolutions and low DoFs. Hu et al. show optimizations for up to 3000 DoFs. Du et al. report gradient computation for up to nearly 30,000 DoFs, whereas our method is capable of computing gradients and perform optimizations with several orders of magnitude increase in DoFs and increased mesh resolutions. Additionally, our method reports faster computation times for similar resolutions and DoFs.

7 DISCUSSION, LIMITATIONS, AND FUTURE WORK

We present an efficient extension to the position-based simulation model of compliant constraint dynamics to obtain gradients with respect to any parameter through a dynamic simulation. We illustrate the effectiveness of the method with several example applications and show that our method is capable of efficiently computing gradients for high resolutions and high DoFs surpassing prior work. Our work focuses on XPBD but it is applicable to PBD as well.

A limitation of the adjoint method is the need to store intermediate particle states and gradients at every time step. The resulting memory usage scales linearly with the length of the simulation. In

practice, this limitation is manageable. Auto-differentiation frameworks typically generate big computational graphs that need to be held in GPU memory which are much more limited compared to modern CPU ram memory. Our approach allows us to store data for individual steps and retrieve them when needed.

Since our contribution does not modify the properties of the forward simulation algorithm, we inherit the same performance advantages but also the limitations such as slow convergence for very stiff constraints.

All optimizations presented were minimized using gradient descent. As future work, we would like to use more complex algorithms such as Limited-memory BFGS or solvers such as Ceres [Agarwal et al. 2022]. Although this is not a limitation of the method, our examples focus on cloth simulations. In the future, we plan to add constraints and their derivatives to enable differentiable simulation of volumetric and strand-level materials in a unified way. Additionally, we are keen to explore end-to-end optimizations from image data by combining differentiable rendering with differentiable simulation.

REFERENCES

Sameer Agarwal, Keir Mierle, and Others. 2022. Ceres Solver. <http://ceres-solver.org>.

David Baraff and Andrew Witkin. 1998. Large steps in cloth simulation. In *Proceedings of the 25th annual conference on Computer graphics and interactive techniques*. 43–54.

Jan Bender, Matthias Müller, and Miles Macklin. 2017. A Survey on Position Based Dynamics. 2017. In *EUROGRAPHICS 2017 Tutorials*. Eurographics Association.

Sofien Bouaziz, Sebastian Martin, Tiantian Liu, Ladislav Kavan, and Mark Pauly. 2014. Projective dynamics: Fusing constraint projections for fast simulation. *ACM transactions on graphics (TOG)* 33, 4 (2014), 1–11.

He Chen, Hyojoon Park, Kutay Macit, and Ladislav Kavan. 2021. Capturing detailed deformations of moving human bodies. *ACM Transactions on Graphics (TOG)* 40, 4 (2021), 1–18.

Hsiao-yu Chen, Edith Tretschk, Tuur Stuyck, Petr Kadlecak, Ladislav Kavan, Etienne Vouga, and Christoph Lassner. 2022. Virtual Elastic Objects. *IEEE Conference on Computer Vision and Pattern Recognition (CVPR) 2022* (2022).

Stelian Coros, Miles Macklin, Bernhard Thomaszewski, and Nils Thürey. 2021. Differentiable Simulation. In *SIGGRAPH Asia 2021 Courses* (Tokyo, Japan) (SA '21). Association for Computing Machinery, New York, NY, USA, Article 3, 142 pages. <https://doi.org/10.1145/3476117.3483433>

Tao Du, Kui Wu, Pingchuan Ma, Sébastien Wah, Andrew Spielberg, Daniela Rus, and Wojciech Matusik. 2021. DiffPFD: Differentiable Projective Dynamics. *ACM Trans. Graph.* 41, 2, Article 13 (nov 2021), 21 pages. <https://doi.org/10.1145/3490168>

Marco Fratarcangeli, Valentina Tibaldo, and Fabio Pellacini. 2016. Vivace: A practical gauss-seidel method for stable soft body dynamics. *ACM Transactions on Graphics (TOG)* 35, 6 (2016), 1–9.

Moritz Geilinger, David Hahn, Jonas Zehnder, Moritz Bächer, Bernhard Thomaszewski, and Stelian Coros. 2020. Add: Analytically differentiable dynamics for multi-body systems with frictional contact. *ACM Transactions on Graphics (TOG)* 39, 6 (2020), 1–15.

Arvi Gjoka, Zizhou Huang, Davi Colli Tozoni, Zachary Ferguson, Teseo Schneider, Daniele Panizzo, and Denis Zorin. 2022. Differentiable solver for time-dependent deformation problems with contact. *arXiv preprint arXiv:2205.13643* (2022).

Jingfan Guo, Jie Li, Rahul Narain, and Hyun Soo Park. 2021. Inverse Simulation: Reconstructing Dynamic Geometry of Clothed Humans via Optimal Control. In *IEEE Conference on Computer Vision and Pattern Recognition (CVPR)*.

David Hahn, Pol Banzet, James M Bern, and Stelian Coros. 2019. Real2Sim: Visco-elastic parameter estimation from dynamic motion. *ACM Transactions on Graphics (TOG)* 38, 6 (2019), 1–13.

Oshri Halimi, Tuur Stuyck, Donglai Xiang, Timur Bagautdinov, He Wen, Ron Kimmel, Takaaki Shiratori, Chenglei Wu, Yaser Sheikh, and Fabian Prada. 2022. Pattern-Based Cloth Registration and Sparse-View Animation. *ACM Trans. Graph.* 41, 6, Article 196 (nov 2022), 17 pages. <https://doi.org/10.1145/3550454.3555448>

Yuanming Hu. 2022. High-performance parallel programming in Python. <https://www.taichi-lang.org/>.

Yuanming Hu, Luke Anderson, Tzu-Mao Li, Qi Sun, Nathan Carr, Jonathan Ragan-Kelley, and Frédéric Durand. 2020. DiffTaichi: Differentiable Programming for Physical Simulation. *ICLR* (2020).

Yuanming Hu, Jiancheng Liu, Andrew Spielberg, Joshua B Tenenbaum, William T Freeman, Jiajun Wu, Daniela Rus, and Wojciech Matusik. 2019. Chainqueen: A real-time differentiable physical simulator for soft robotics. In *2019 International conference on robotics and automation (ICRA)*. IEEE, 6265–6271.

Krishna Murthy Jatavallabhula, Miles Macklin, Florian Golemo, Vikram Voleti, Linda Petrini, Martin Weiss, Breandan Considine, Jerome Parent-Levesque, Kevin Xie, Kenny Erleben, Liam Paull, Florian Shkurti, Derek Nowrouzezahrai, and Sanja Fidler. 2021. gradSim: Differentiable simulation for system identification and visuomotor control. *International Conference on Learning Representations (ICLR)* (2021). https://openreview.net/forum?id=c_E8kFWfhp0

Theodore Kim and David Eberle. 2022. Dynamic deformables: implementation and production practicalities (now with code!). In *ACM SIGGRAPH 2022 Courses*. 1–259.

Egor Larionov, Marie-Lena Eckert, Katja Wolff, and Tuur Stuyck. 2022. Estimating Cloth Elasticity Parameters Using Position-Based Simulation of Compliant Constrained Dynamics. *arXiv preprint arXiv:2212.08790* (2022).

Yifei Li, Tao Du, Kui Wu, Jie Xu, and Wojciech Matusik. 2022. DiffCloth: Differentiable Cloth Simulation with Dry Frictional Contact. *ACM Trans. Graph.* 42, 1, Article 2 (oct 2022), 20 pages. <https://doi.org/10.1145/3527660>

Junbang Liang, Ming Lin, and Vladlen Koltun. 2019. Differentiable cloth simulation for inverse problems. *Advances in Neural Information Processing Systems* 32 (2019).

Matthew Loper, Naureen Mahmood, Javier Romero, Gerard Pons-Moll, and Michael J. Black. 2015. SMPL: A Skinned Multi-Person Linear Model. *ACM Trans. Graphics (Proc. SIGGRAPH Asia)* 34, 6 (Oct. 2015), 248:1–248:16.

Miles Macklin. 2022. Warp: A High-performance Python Framework for GPU Simulation and Graphics. <https://github.com/nvidia/warp>. NVIDIA GPU Technology Conference (GTC).

Miles Macklin, Matthias Müller, and Nuttapon Chentanez. 2016. XPBD: position-based simulation of compliant constrained dynamics. In *Proceedings of the 9th International Conference on Motion in Games*. 49–54.

Antoine McNamara, Adrien Treuille, Zoran Popović, and Jos Stam. 2004. Fluid control using the adjoint method. *ACM Transactions On Graphics (TOG)* 23, 3 (2004), 449–456.

Eder Miguel, Derek Bradley, Bernhard Thomaszewski, Bernd Bickel, Wojciech Matusik, Miguel A. Otaduy, and Steve Marschner. 2012. Data-Driven Estimation of Cloth Simulation Models. *Computer Graphics Forum* 31, 2pt2 (2012), 519–528. <https://doi.org/10.1111/j.1467-8659.2012.03031.x> arXiv:<https://onlinelibrary.wiley.com/doi/pdf/10.1111/j.1467-8659.2012.03031.x>

Ben Mildenhall, Pratul P Srinivasan, Matthew Tancik, Jonathan T Barron, Ravi Ramamoorthi, and Ren Ng. 2021. Nerf: Representing scenes as neural radiance fields for view synthesis. *Commun. ACM* 65, 1 (2021), 99–106.

Matthias Müller, Bruno Heidelberger, Marcus Hennix, and John Ratcliff. 2007. Position based dynamics. *Journal of Visual Communication and Image Representation* 18, 2 (2007), 109–118.

Yi-Ling Qiao, Junbang Liang, Vladlen Koltun, and Ming C. Lin. 2020. Scalable Differentiable Physics for Learning and Control. In *ICML*.

Michael Strecke and Jörg Stückler. 2021. DiffSDFSim: Differentiable Rigid-Body Dynamics With Implicit Shapes. In *International Conference on 3D Vision (3DV)*.

Tuur Stuyck. 2018. Cloth simulation for computer graphics. *Synthesis Lectures on Visual Computing: Computer Graphics, Animation, Computational Photography, and Imaging* 10, 3 (2018), 1–121.

Rasmus Tamstorf, Toby Jones, and Stephen F McCormick. 2015. Smoothed aggregation multigrid for cloth simulation. *ACM Transactions on Graphics (TOG)* 34, 6 (2015), 1–13.

Huamin Wang, James F O'Brien, and Ravi Ramamoorthi. 2011. Data-driven elastic models for cloth: modeling and measurement. *ACM transactions on graphics (TOG)* 30, 4 (2011), 1–12.

Sebastian Weiss, Robert Maier, Daniel Cremers, Rudiger Westermann, and Nils Thuerey. 2020. Correspondence-free material reconstruction using sparse surface constraints. In *Proceedings of the IEEE/CVF Conference on Computer Vision and Pattern Recognition*. 4686–4695.

Ryan White, Keenan Crane, and D. A. Forsyth. 2007. Capturing and animating occluded cloth. *ACM Trans. Graph.* 26 (July 2007), Issue 3.

Chris Wojtan, Peter J Mucha, and Greg Turk. 2006. Keyframe control of complex particle systems using the adjoint method. In *Proceedings of the 2006 ACM SIGGRAPH/Eurographics symposium on Computer animation*. 15–23.